Notes on semi-implicit time stepping, blended models, etc.

T. Benacchio, MetOffice, Exeter, UK
R. Klein, Mathematics & Informatics, Freie Universität Berlin

November 9, 2016

1 Introduction

Previous attempts at implementing the semi-implicit time discretization strategy as explicated in T. Benacchio's thesis have not allowed us to go to time steps larger than $N\Delta t$, where N is the Brunt-Väisälä frequency and Δt the time step. It seems that it is necessary to split advection of potential temperature, θ, into that of its large-scale horizontal mean, $\overline{\theta}$, and deviations, $\widetilde{\theta}$, from it. Advection of the former becomes part of the (quasi-)linearized implicity system and that of the latter remains part of the explicit advection step. This corresponds to the usual practice of subtracting out a background profile of θ at the differential equation level. A dynamically evolving and horizontally non-homogeneous background can be thought of in terms of a multiscale/multigrid strategy, but we leave this for later.

The time stepping strategy to be described here follows closely that described by P. Smolarkiewicz in a series of papers, see, e.g., (Smolarkiewicz et al. 2014, Smolarkiewicz & Margolin 1998).

2 Getting rid of the first (MAC) projection

2.1 Node- and cell-centered divergences

Currently, our scheme invokes two sequential projections / Helmholtz-solves to realize consistent divergence of the advective fluxes $P\boldsymbol{v}$. The first fixes the actual flux divergence employed in discretizing the advection terms, the second makes sure that the cell centered velocities are compatible with the respective constraint as well.

Two elliptic solves are expensive, so the question naturally arises as to whether there is a way to eliminate one of them. Here is a suggestion for how to achieve this without losing second-order accuracy. This suggestion is partially inspired by the time stepping and spatial discretization strategy of Piotr Smolarkiewicz' EULAG code (see, e.g., Smolarkiewicz & Margolin 1998).

The key observation can be explained on the basis of Fig. 1. The "second projection" in the current setting involves a discrete divergence for each node (filled squares in Fig. 1), *i.e.*, for some vector field $\boldsymbol{v} = (u, v)^t$ we have

$$\widetilde{(\nabla \cdot \boldsymbol{v})}_{i+\frac{1}{2},j+\frac{1}{2}} = \frac{(u_{i+1,j} + u_{i+1,j+1}) - (u_{i,j} + u_{i,j+1})}{2\Delta x} + \frac{(v_{i,j+1} + v_{i+1,j+1}) - (v_{i+1,j} + v_{i,j})}{2\Delta y}. \quad (1)$$

Now we observe that averaging these divergences over the four dual cells that overlap with cell (i, j), we obtain a valid divergence discretization for that cell,

$$\frac{1}{4}\left(\widetilde{(\nabla \cdot \boldsymbol{v})}_{i+\frac{1}{2},j+\frac{1}{2}} + \widetilde{(\nabla \cdot \boldsymbol{v})}_{i-\frac{1}{2},j+\frac{1}{2}} + \widetilde{(\nabla \cdot \boldsymbol{v})}_{i-\frac{1}{2},j-\frac{1}{2}} + \widetilde{(\nabla \cdot \boldsymbol{v})}_{i+\frac{1}{2},j-\frac{1}{2}}\right) = \overline{(\nabla \cdot \boldsymbol{v})}_{i,j} \quad (2)$$

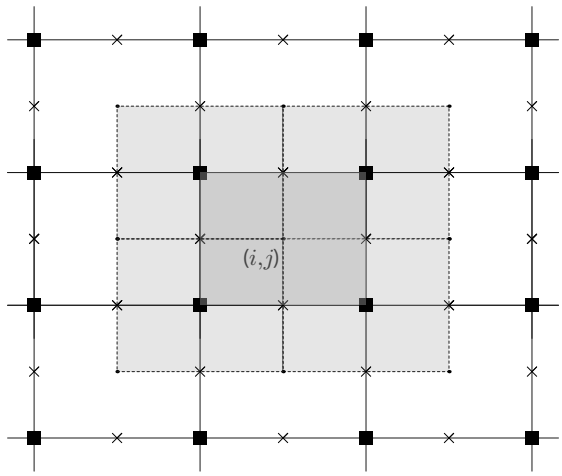

Figure 1: Arrangement of primary and dual cells surrounding a reference cell (i, j) on a cartesian 2D mesh.

where

$$\overline{(\nabla \cdot \boldsymbol{v})}_{i,j} = \frac{\overline{u}_{i+\frac{1}{2},j} - \overline{u}_{i-\frac{1}{2},j}}{\Delta x} + \frac{\overline{v}_{i,j+\frac{1}{2}} - \overline{v}_{i,j-\frac{1}{2}}}{\Delta y} \tag{3}$$

with the averaged primary cell interface velocities

$$\begin{aligned} \overline{u}_{i+\frac{1}{2},j} &= \frac{1}{8}\Big([u_{i+1,j+1} + 2u_{i+1,j} + u_{i+1,j-1}] + [u_{i,j+1} + 2u_{i,j} + u_{i,j-1}]\Big) \\ \overline{v}_{i,j+\frac{1}{2}} &= \frac{1}{8}\Big([v_{i+1,j+1} + 2v_{i,j+1} + v_{i-1,j+1}] + [v_{i+1,j} + 2v_{i,j} + v_{i-1,j}]\Big) \, . \end{aligned} \tag{4}$$

We conclude that from the dual cell discrete divergence we can readily construct a compatible primary cell discrete divergence in conseration form. This is the key in replacing the MAC-projection of the scheme.

2.2 Outline of modified divergence control

The advecting fluxes $(P\boldsymbol{v})^{n+\frac{1}{2}}$ should ideally be determined using the implicit trapezoidal rule so that

$$(P\boldsymbol{v})^{n+\frac{1}{2}} = \frac{1}{2}\left((P\boldsymbol{v})^{n} + (P\boldsymbol{v})^{n+1}\right) \, . \tag{5}$$

1. Store the cellface advective fluxes at time level n based on (4) in two separate fields. The first is to keep this quantity, the second is to be modified in the course of a time step to bring it to the new time level. Let us denote these fields by $(P\boldsymbol{v})^{n}$ and $(P\boldsymbol{v})^{n+\xi}$

2. Run the explicit predictor as before with the only exception of how the advective fluxes are determined in the flux function. Instead of directly letting, e.g., in the first x-step,

$$(Pu)^{n+\xi_1}_{i+\frac{1}{2},j} = \frac{1}{2}\left((Pu)^{n+\xi_1}_{i^+,j} + (Pu)^{n+\xi_1}_{[i+1]^-,j}\right) \tag{6}$$

with $[\cdot]_{i^+,j}$ denoting reconstructed states at the split-step half time level at the right edge of primary cell (i,j), we let

$$(Pu)_{i+\frac{1}{2},j}^{n+\xi_{m+1}} = (Pu)_{i+\frac{1}{2},j}^{n+\xi_m} + \widetilde{\Delta\,(Pu)}_{i+\frac{1}{2},j}^{n+\xi_{m+1}} \tag{7}$$

with the increment obtained from the local MUSCL-type reconstruction as

$$\begin{aligned} \widetilde{\Delta\,(Pu)}_{i+\frac{1}{2},j}^{n+\xi_{m+1}} &= \frac{1}{4}\left((Pu)_{i^+,j} + (Pu)_{i^-,j} + (Pu)_{[i+1]^-,j} + (Pu)_{[i+1]^+,j}\right)^{n+\xi_{m+1}} \\ &\quad -\frac{1}{2}\left((Pu)_{i,j} + (Pu)_{[i+1],j}\right)^{n+\xi_m} \end{aligned} \tag{8}$$

3. Once the predictor is done the advective fluxes in the second auxiliary field have been updated provisionally using the explicit scheme to time level $t^{n+\frac{1}{2}}$, which are labelled

$$(Pu)_{i+\frac{1}{2},j}^{n+\frac{1}{2},\nu}, \quad (Pu)_{i,j+\frac{1}{2}}^{n+\frac{1}{2},\nu}. \tag{9}$$

   To start the divergence correction iterations, let $\nu = 0$.

4. Next we want a divergence-controlled velocity field at t^{n+1}. To this end, run the second projection for the cell-centered fields. From the corrected $(P\boldsymbol{v})_{i,j}^{n+1,\nu}$ field, compute advecting fluxes at the cell faces using (4). This generates the fields

$$(Pu)_{i+\frac{1}{2},j}^{n+1,\nu}, \quad (Pu)_{i,j+\frac{1}{2}}^{n+1,\nu}. \tag{10}$$

5. From these, and the old time level advective fluxes we obtain the next iterate for the half-time advective fluxes

$$(P\boldsymbol{v})^{n+\frac{1}{2},\nu+1} = \frac{1}{2}\left((P\boldsymbol{v})^{n+1,\nu} + (P\boldsymbol{v})^{n}\right) \tag{11}$$

6. The νth correction cycle is completed by running the advection correction based on the advective flux increments

$$\Delta(P\boldsymbol{v})^{n+\frac{1}{2},\nu} = (P\boldsymbol{v})^{n+\frac{1}{2},\nu+1} - (P\boldsymbol{v})^{n+\frac{1}{2},\nu}. \tag{12}$$

7. Check convergence and either continue the iteration or stop.

8.

9. Run the scheme as before up until the first projection would be invoked, except that the advecting fluxes are now computed using the averaging formulae in (4). Also, the effective advective fluxes over the entire advection cycle (be it computed via OpSplit or RK) are to be monitored. This yields advective fluxes $(Pu)_{i+\frac{1}{2},j}^{\nu,n+\frac{1}{2}}$ and $(Pv)_{i,j+\frac{1}{2}}^{\nu,n+\frac{1}{2}}$ for $\nu = 0$.

10. Run the node-centered projection to obtain the next iterate of the divergence corrected cell-centered velocities. Compute first iterate target cell interface advective fluxes using (4), $(Pu)_{i+\frac{1}{2},j}^{\nu+1,n+\frac{1}{2}}$ and $(Pv)_{i,j+\frac{1}{2}}^{\nu+1,n+\frac{1}{2}}$.

11. Correct advection results based on the advecting flux differences $(Pu)_{i+\frac{1}{2},j}^{\nu+1,n+\frac{1}{2}} - (Pu)_{i+\frac{1}{2},j}^{\nu,n+\frac{1}{2}}$ and $(Pv)_{i,j+\frac{1}{2}}^{\nu+1,n+\frac{1}{2}} - (Pv)_{i,j+\frac{1}{2}}^{\nu,n+\frac{1}{2}}$.

12. If $\| (P\boldsymbol{v})^{\nu+1,n+\frac{1}{2}} - (P\boldsymbol{v})^{\nu,n+\frac{1}{2}} \| \geq \text{tol}$ return to step 10, else we are done.

3 The time stepping strategy

Let U denote our vector of unknowns, which are generally conserved quantities in the standard sense, except maybe for the energy variable. Here we use $P = \rho\theta$ for energy as in (Benacchio et al. 2014, Klein 2009), where ρ is the density. Thus,

$$U = \begin{pmatrix} \rho \\ \rho \boldsymbol{v} \\ P \end{pmatrix} \tag{13}$$

where $\boldsymbol{v}$ is the velocity. These unknowns depend on time t, horizontal position $\boldsymbol{x} = (x, y)$ and vertical position z, *i.e.*, we have the signature $U(t, \boldsymbol{x}, z)$.

We cover compressible and pseudo-incompressible flow following (Durran 1989) through the blended evolution equation (Benacchio et al. 2014)

$$D_\alpha U_t = \mathcal{A}[U] + \mathcal{R}[U] \tag{14}$$

with

$$D_\alpha = \begin{pmatrix} 1 & 0 & 0 \\ 0 & \mathrm{Id} & 0 \\ 0 & 0 & \alpha \end{pmatrix}, \quad \mathcal{A}[\rho\psi] = -\nabla \cdot (P\boldsymbol{v}[\psi/\theta]), \quad \mathcal{R}[U] = \begin{pmatrix} 0 \\ \nabla p' - g\boldsymbol{k}\left(\rho + \frac{1-\alpha}{c_0^2} p'\right) \\ \rho S(\theta) \end{pmatrix}. \tag{15}$$

Here $\alpha \in [0, 1]$ and the system describes fully compressible flow for $\alpha = 1$ and pseudo-incompressible flow for $\alpha = 0$. The quantities $\overline{c}_0$ and p' are defined once a horizontally homogeneous background stratification $(P_0, \rho_0, \theta_0)(z)$ of the thermodynamic variables has been defined. To this end we pick, e.g., a background potential temperature distribution $\theta_0(z)$ and then obtain P_0 and ρ_0 assuming hydrostatic balance, *i.e.*,

$$\frac{dp_0}{dz} = -\rho_0 g\,, \qquad p_0 = P_0^{1/\gamma}\,, \qquad \rho_0 = \frac{P_0}{\theta_0}\,, \qquad P_0(0) = 1\,, \tag{16}$$

where γ is the isentropic exponent which is assumed to be constant here. Then we have

$$c_0^2 = \gamma \frac{p_0}{\rho_0}\,, \qquad \text{and} \qquad p' = P^{1/\gamma} - P_0^{1/\gamma} \quad (\alpha \neq 0)\,. \tag{17}$$

For the limiting pseudo-incompressible case, $\alpha = 0$, p' cannot be obtained from the primary thermodynamic variables but satisfies an elliptic equation that guarantees compliance of the velocity field with the pseudo-incompressible divergence constraint $\nabla \cdot (P_0 \boldsymbol{v}) = \rho S(\theta)$.

then a second-order time stepping strategy reads

$$D_\alpha U^{n+1} = \widetilde{\mathcal{A}}\left[D_\alpha U^n + \frac{\Delta t}{2}\mathcal{R}[U^n]\right] + \mathcal{R}\left[U^{n+1}\right]\,. \tag{18}$$

4 Semi-implicit gravity

To be solved in a (linearized) implicit, backward Euler step over $\Delta t/2$,

$$w_t = -\frac{\theta}{\Gamma}(\pi_z + \Gamma g \chi) \tag{19}$$

$$\chi_t = -w\frac{d\overline{\chi}}{dz} \tag{20}$$

where $\theta = 1/\chi$ is frozen in the linearization. The current state is w^*, χ^*, π^*.
Then, an implicit step over time step Δt reads

$$w^{n+1} - w^* = \delta w = -\Delta t \frac{\theta}{\Gamma} \left([\pi^* + \delta\pi]_z + \Gamma g [\chi^* + \delta\chi] \right) \tag{21}$$

$$\chi^{n+1} - \chi^* = \delta\chi = -\Delta t \, (w^* + \delta w) \frac{d\overline{\chi}}{dz} \, . \tag{22}$$

Reorder explicit and implicit contributions, replace $\delta\chi$ in (21) and solve for δw,

$$w^{n+1} - w^* = \delta w = -\Delta t \frac{\theta}{\Gamma} (\pi_z^* + \Gamma g \chi^*) - \Delta t \frac{\theta}{\Gamma} (\delta\pi_z + \Gamma g \delta\chi) \tag{23}$$

$$= -\Delta t \frac{\theta}{\Gamma} (\pi_z^* + \Gamma g \chi^*) - \Delta t \frac{\theta}{\Gamma} \left(\delta\pi_z - \Delta t \, \Gamma g (w^* + \delta w) \frac{d\overline{\chi}}{dz} \right) \tag{24}$$

$$\delta w \left(1 - (\Delta t)^2 g\theta \frac{d\overline{\chi}}{dz} \right) = -\Delta t \frac{\theta}{\Gamma} (\pi_z^* + \Gamma g \chi^*) + w^* (\Delta t)^2 g\theta \frac{d\overline{\chi}}{dz} - \Delta t \frac{\theta}{\Gamma} \delta\pi_z \, . \tag{25}$$

Letting

$$N_{sc}^2 = -(\Delta t)^2 g\theta \frac{d\overline{\chi}}{dz} \tag{26}$$

we have

$$\delta w = \frac{1}{1 + N_{sc}^2} \left(-\Delta t \frac{\theta}{\Gamma} (\pi_z^* + \Gamma g \chi^*) - w^* N_{sc}^2 \right) - \Delta t \frac{\theta/\Gamma}{1 + N_{sc}^2} \delta\pi_z \tag{27}$$

and the update formular for χ subsequently follows from (22).
In (28) we use the abbreviation $\Gamma g \chi^* = -\pi_z^{\mathrm{hy}}$ to obtain

$$\delta w = \frac{1}{1 + N_{sc}^2} \left(-\Delta t \frac{\theta}{\Gamma} \left(\pi_z^* - \pi_z^{\mathrm{hy}} \right) - w^* N_{sc}^2 \right) - \Delta t \frac{\theta/\Gamma}{1 + N_{sc}^2} \delta\pi_z \tag{28}$$

$$\delta w = \delta^{\mathrm{expl}} w + \delta^{\pi} w \tag{29}$$

$$\delta\chi = -\Delta t \, (w^* + \delta^{\mathrm{expl}} w) \frac{d\overline{\chi}}{dz} + \frac{1}{\Gamma g} \frac{1}{1 + N_{sc}^2} (\Delta t)^2 g\theta \frac{d\overline{\chi}}{dz} \delta\pi_z \tag{30}$$

$$\delta\chi = -\Delta t \, (w^* + \delta^{\mathrm{expl}} w) \frac{d\overline{\chi}}{dz} + \frac{1}{\Gamma g} \frac{N_{sc}^2}{1 + N_{sc}^2} \delta\pi_z \tag{31}$$

References

Benacchio T, O'Neill W, Klein R. 2014. A blended soundproof-to-compressible model for atmospheric dynamcis. *Mon. Wea. Rev.* 142:4416–4438

Durran DR. 1989. Improving the anelastic approximation. *Journal of Atmosphere Sciences* 46:1453–1461

Klein R. 2009. Asymptotics, Structure, and Integration of Sound-Proof Atmospheric flow Equations. *Theoretical and Computational Fluid Dynamics* 23:161–195

Smolarkiewicz P, Kühnlein C, Wedi N. 2014. A consistent framework for discrete integrations of soundproof and compressible PDEs of atmospheric dynamics. *J. Comput. Phys.* 263:185–205

Smolarkiewicz PK, Margolin LG. 1998. Mpdata: A finite-difference solver for geophysical flows. *J. Comp. Phys.* 140:459–480